Multi-Frame Track-Before-Detect Method of Airborne Multi-channel Radar in Weak Moving Target Detection

Runming Zou, Hao Wu, Yongqiang Cheng, Xiaoqiang Hua, Zheng Yang
Kang Liu, Hongqiang Wang
College of Electronic Science and Technology
National University of Defense Technology
Changsha, China
nudtzrm@163.com, wu_hao_95@163.com, nudtyqcheng@gmail.com, hxq712@yeah.net, yangzheng18a@163.com
liukang117@126.com, oliverwhq@tom.com

***Abstract*—To address the problem of weak target detection, this paper proposes a information geometry-based multi-frame track-before-detect (TBD) method to implement the multi-frame integration and enhance the target detection performance. Specifically, a space-time adaptive detector based on hermitian positive definite (HPD) matrix manifold is proposed to improve the detection performance of weak target in heterogeneous environments. Then, to integrate the inter-frame target information, we apply this detector to TBD and propose a dynamic programming (DP) algorithm which obeys Doppler constraint rather than the ordinary maximum speed constraint. As a consequence, an information geometry-based DP-TBD method is developed, which has better detection performance for weak targets in heterogeneous strong clutter environment. The advantages of the proposed method are validated by the experiments utilizing real radar data.**

***Index Terms*—information geometry, track before detection, radar target detection, airborne multi-channel radar.**

I. Introduction

The airborne multi-channel radars are widely used in the marine surveillance and weak target detection [1]–[3]. To overcome the clutter spectrum broadening problem, the space-time adaptive detector is studied and applied to airborne multi-channel radars. The detectability generally depends on the target's signal-to-clutter ratio (SCR). However, airborne radar usually works in a strongly cluttered environment, and the clutter is heterogeneous, causing low SCR radar returns and severe detection performance degradation [4]–[6].

The adaptive detector for multi-channel radar was first investigated in [7]. Then, many other detectors such as adaptive matched filter (AMF) [8] and normalized adaptive matched filter (ANMF) [9] were proposed to integrate intra-frame target information [10]. However, these intra-frame integration methods rely much on the energy feature of the target and are greatly affected by the resident time of the motion target and the heterogeneous strong clutter in practice.

In addition to the intra-frame detection methods, the multi-frame detection approaches are extensively concerned for their outstanding performance in weak target detection [11]. The multi-frame TBD, which processes the un-thresholded data, is widely recognized as an effective method [12]–[16]. TBD algorithms include the particle filter TBD (PF-TBD) [17], the Hough transform TBD (HT-TBD) [18] and the dynamic programming TBD [19] etc. Unlike the PF-TBD, the DP-TBD does not rely on the target's state and motion equations but transforms the multi-frame detection problem into a multi-stage decision optimization problem. The DP-TBD regards the processing result of each frame as a sub-stage and outputs the target trajectory by accumulating the detection results of different sub-stages. Therefore, unlike the HT-TBD, the DP-TBD method is not constrained by the target motion model. As a result of the advantages mentioned above, the DP-TBD algorithm is widely used to detect weak and highly mobile targets, including unmanned aerial vehicles (UAVs), motorboats, and so on. However, in heterogeneous environments and clutter environments, the energy features of the target and clutter are not distinguishable, posing challenges for target detection. As analyzed above, whether intra-frame detection or multi-frame integration suffers the heterogeneous clutter and low SCR target.

Recently, related research on the information geometry-based radar target detection method has gained a lot of attention due to its distinctive advantages in weak target detection, especially for targets in heterogeneous and strong clutter environments [20]–[23]. Benefiting from the excellent ability to distinguish targets from clutter on the matrix manifold, the matrix information geometry (MIG) detector performs well in weak target detection. In this paper, we propose a novel space-time adaptive detector based on information geometry to improve the intra-frame detection performance and apply the proposed detector to multi-frame DP-TBD. Since the proposed detector utilizes the geometric features on the hermitian

This work was supported by the National Key Research and Development Program of China under Grant 2022YFB3902400, the Distinguished Youth Science Foundation of Hunan Province under Grant 2022JJ10063, and the National Natural Science Foundation of China under Grant 62322122, 61921001 and 62371458.

positive definite (HPD) matrix manifold to distinguish the target from clutter, it performs better in heterogeneous and strong clutter environments. Meanwhile, the target Doppler information is exploited in DP-TBD to obtain a more accurate target trajectory, thus the performance of multi-frame detection is also improved. The main contributions are listed as follows.

- A novel space-time adaptive detector is proposed. The proposed detector is derived from the Kullback–Leibler divergence (KLD) between matrices on the HPD manifold and achieves better detection performance.
- A DP-TBD method based on the proposed detector is developed. The proposed DP-TBD method obey the Doppler constraint rather than the conventional maximum speed constraint in target detection, therefore it has better detection and track performance.
- We present experiment results of real measured data to evaluate the detection performance advantages of the proposed method.

II. Signal Model and Problem Formulation

Consider a side-looking airborne uniform liner array radar constructed by N antenna elements. Assuming that each antenna receives P pulses in a coherent processing interval (CPI). The degree of freedom (DoF) of this airborne radar system is $M = NP$. Then the received signal in a range cell $\boldsymbol{x} \in \mathbb{C}^M$ can be formulated as

$$\boldsymbol{x} = \alpha_{\mathrm{t}} \boldsymbol{s}_{\mathrm{t}} + \boldsymbol{x}_{\mathrm{c}} + \boldsymbol{n} \tag{1}$$

where $\boldsymbol{x}_{\mathrm{c}}$ and $\boldsymbol{n} \sim N(0, \sigma_n^2)$ are the clutter and noise respectively. Unknown variables α_{t} and given vector $\boldsymbol{s}_{\mathrm{t}}$ respectively are the reflection coefficient and steering vector of the target.

The received clutter of airborne radar can be modeled as the superposition of the clutter patches in the radar main lobe, namely,

$$\boldsymbol{x}_{\mathrm{c}} = \sum_{i=1}^{N_{\mathrm{c}}} \alpha_i \boldsymbol{s}_i \tag{2}$$

where N_{c} is the number of clutter patches, α_i and $\boldsymbol{s}_i$ respectively are the reflection coefficient and steering vector of the i^{th} clutter patch.

Based on the clutter signal model introduced above, the detection problem for airborne radar can be formulated by the following binary hypothesis testing problem

$$\begin{aligned} \mathcal{H}_0 &: \begin{cases} \boldsymbol{x}_{\mathrm{CUT}} = \boldsymbol{x}_{\mathrm{c}} + \boldsymbol{n}, \\ \boldsymbol{x}_i = \boldsymbol{x}_{\mathrm{c}i} + \boldsymbol{n}, \quad i = 1, \ldots, n \end{cases} \\ \mathcal{H}_1 &: \begin{cases} \boldsymbol{x}_{\mathrm{CUT}} = \alpha_{\mathrm{t}} \boldsymbol{s}_{\mathrm{t}} + \boldsymbol{x}_{\mathrm{c}} + \boldsymbol{n}, \\ \boldsymbol{x}_i = \boldsymbol{x}_{\mathrm{c}i} + \boldsymbol{n}, \quad i = 1, \ldots, n \end{cases} \end{aligned} \tag{3}$$

where $\boldsymbol{x}_{\mathrm{CUT}}$ is the echo of the cell under test (CUT). $\boldsymbol{x}_i$ and $\boldsymbol{x}_{ci}$ respectively are the received echo and clutter in i^{th} range cell. n is the number of reference samples which are adjacent to the CUT.

In statistical signal processing, the generalized likelihood ratio test (GLRT) is a basic form of hypothesis testing. The GLRT of multi-channel radar signal on the HPD manifold is derived as the following equation [24].

$$l = \mathcal{D}_{\mathrm{KL}}(\mathbf{R}_{\mathrm{CUT}}, \mathbf{R}_{\mathrm{c}}) - \mathcal{D}_{\mathrm{KL}}(\mathbf{R}_{\mathrm{CUT}}, \mathbf{R}_{\mathrm{c}} + \mathbf{R}_{\mathrm{t}}) \underset{\mathcal{H}_0}{\overset{\mathcal{H}_1}{\gtrless}} \eta \tag{4}$$

where l is the normalized log-likelihood ratio, η is the detection threshold. Matrices $\mathbf{R}_{\mathrm{CUT}}$, $\mathbf{R}_{\mathrm{c}}$ and $\mathbf{R}_{\mathrm{t}} = \alpha_{\mathrm{t}} \alpha_{\mathrm{t}}^{\mathrm{H}} \boldsymbol{s}_{\mathrm{t}} \boldsymbol{s}_{\mathrm{t}}^{\mathrm{H}}$ respectively denote the covariance of the CUT, clutter and target. $\mathcal{D}_{\mathrm{KL}}$ is the KLD between matrices and is calculated by

$$\mathcal{D}_{\mathrm{KL}}(\mathbf{P}, \mathbf{Q}) = \mathrm{tr}(\mathbf{P}^{-1}\mathbf{Q}) - \log \left| \mathbf{P}^{-1}\mathbf{Q} \right| - M \tag{5}$$

Therefore formula (4) is equal to

$$\begin{aligned} l =& \mathrm{tr}(\mathbf{R}_{\mathrm{CUT}}^{-1} \mathbf{R}_{\mathrm{c}}) - \log(|\mathbf{R}_{\mathrm{CUT}}^{-1} \mathbf{R}_{\mathrm{c}}|) \\ & - \mathrm{tr}(\mathbf{R}_{\mathrm{CUT}}^{-1} (\mathbf{R}_{\mathrm{c}} + \mathbf{R}_{\mathrm{t}})) + \log(|\mathbf{R}_{\mathrm{CUT}}^{-1} (\mathbf{R}_{\mathrm{c}} + \mathbf{R}_{\mathrm{t}})|) \\ =& - \mathrm{tr}(\mathbf{R}_{\mathrm{CUT}}^{-1} \mathbf{R}_{\mathrm{t}}) + \log(|\mathrm{R}_{\mathrm{CUT}}^{-1} (\mathrm{R}_{\mathrm{c}} + \mathrm{R}_{\mathrm{t}})|) \\ & - \log(|\mathrm{R}_{\mathrm{CUT}}^{-1} \mathrm{R}_{\mathrm{c}}|) \underset{\mathcal{H}_0}{\overset{\mathcal{H}_1}{\gtrless}} \eta \end{aligned} \tag{6}$$

III. The Proposed Method

A. The Proposed Space-time Adaptive Detector

In this paper, we give a review of formula (1) and (2), the received signal of multi-channel radar can be reformulated as

$$\boldsymbol{x} = \mathrm{D} \boldsymbol{\gamma} + \boldsymbol{n} \tag{7}$$

where $\mathrm{D} = [\boldsymbol{s}_1 \, \boldsymbol{s}_2 \cdots \boldsymbol{s}_{N_c}] \in \mathbb{C}^{M \times N_c}$ is the coordinate matrix composed of steering vectors and reflection coefficient vector $\boldsymbol{\gamma} = [\alpha_1 \, \alpha_2 \cdots \alpha_{N_c}]^{\mathrm{T}}$.

In practice, the number of clutter patches N_c is not given and ought to be estimated. In addition, the steering vectors $\boldsymbol{s}_i \in \mathrm{D}$, $i = 1 \cdots N_c$ are unknown. To avoid this problem, a feasible and widely accepted method is that the steering vectors in coordinate matrix can be obtained by uniformly discretizing the normalized space–time plane into NP grid points and then each grid point is associated with a space–time steering vector [25]. Although the obtained steering vectors are not completely consistent with the actual situation, the steering vector of the real clutter patches can be reasonable represented by a highly correlated steering vector in D_0 from a mathematical point of view.

Noted that the steering vectors obtained by the method mentioned above are orthorhombic to each other [25], we have $N_c = NP = M$. Then, the covariance matrix of the clutter and noise can be expressed as

$$\begin{aligned} \mathrm{R} =& \, \mathrm{R}_{\mathrm{c}} + \mathrm{R}_{\mathrm{n}} \\ =& \, \mathrm{E}[\boldsymbol{x}_{\mathrm{c}} \boldsymbol{x}_{\mathrm{c}}^{\mathrm{H}}] + \mathrm{E}[\boldsymbol{n}\boldsymbol{n}^{\mathrm{H}}] \\ =& \, \mathrm{D} \boldsymbol{\Lambda}(\boldsymbol{\gamma}) \mathrm{D}^{\mathrm{H}} + \sigma_n^2 \mathrm{I} \\ =& \, \mathrm{D}_{\perp} \begin{bmatrix} \alpha_1^2 + \frac{1}{M}\sigma_n^2 & \cdots & 0 \\ 0 & \ddots & 0 \\ 0 & 0 & \alpha_M^2 + \frac{1}{M}\sigma_n^2 \end{bmatrix} \mathrm{D}_{\perp}^{\mathrm{H}} \end{aligned} \tag{8}$$

where symbol $\mathrm{E}[\cdot]$ denotes the mathematical expection, $\boldsymbol{\Lambda}(\boldsymbol{\gamma})$ is the the diagonal matrix constructed by the square of vector

$$
\begin{aligned}
|\mathrm{R}_{\mathrm{CUT}}^{-1}(\mathrm{R}_{\mathrm{c}}+\mathrm{R}_{\mathrm{t}})| &= \frac{M(\alpha_{\mathrm{t}}^2+\alpha_{\mathrm{c}(i)}^2)+\sigma_n^2}{M\alpha_{\mathrm{cut}(t)}^2+\sigma_n^2}\prod_{i=1,i\neq t}^{M}\frac{M\alpha_{\mathrm{c}(i)}^2+\sigma_n^2}{M\alpha_{\mathrm{cut}(i)}^2+\sigma_n^2} \\
\mathrm{tr}(\mathrm{R}_{\mathrm{CUT}}^{-1}(\mathrm{R}_{\mathrm{c}}+\mathrm{R}_{\mathrm{t}})) &= \sum_{i=1}^{M}\frac{M\alpha_{\mathrm{c}(i)}^2+\sigma_n^2}{M\alpha_{\mathrm{cut}(i)}^2+\sigma_n^2}+\frac{M\alpha_{\mathrm{t}}^2}{M\alpha_{\mathrm{cut}(t)}^2+\sigma_n^2}
\end{aligned} \tag{11}
$$

$\boldsymbol{\gamma}$, and $\mathrm{D}_\perp = \frac{1}{\sqrt{M}}\mathrm{D}$ is the normalized orthogonal coordinate matrix.

Arrange that the reflection coefficient vector of the CUT and clutter range cell respectively are $\gamma_{\mathrm{cut}} = [\alpha_{\mathrm{cut}(1)}\alpha_{\mathrm{cut}(2)}\cdots\alpha_{\mathrm{cut}(M)}]^{\mathrm{T}}$ and $\gamma_{\mathrm{c}} = [\alpha_{\mathrm{c}(1)}\alpha_{\mathrm{c}(2)}\cdots\alpha_{\mathrm{c}(M)}]^{\mathrm{T}}$, applying (8), we have

$$
\mathrm{R}_{\mathrm{CUT}}^{-1}\mathrm{R}_{\mathrm{c}} = \mathrm{D}_\perp\begin{bmatrix} \frac{M\alpha_{\mathrm{c}(1)}^2+\sigma_n^2}{M\alpha_{\mathrm{cut}(1)}^2+\sigma_n^2} & \cdots & 0 \\ 0 & \ddots & 0 \\ 0 & 0 & \frac{M\alpha_{\mathrm{c}(M)}^2+\sigma_n^2}{M\alpha_{\mathrm{cut}(M)}^2+\sigma_n^2}\end{bmatrix}\mathrm{D}_\perp^{\mathrm{H}} \tag{9}
$$

Obviously, formula (9) obeys the form of the eigenvalue decomposition of matrix, thus

$$
\begin{aligned}
|\mathrm{R}_{\mathrm{CUT}}^{-1}\mathrm{R}_{\mathrm{c}}| &= \prod_{i=1}^{M}\frac{M\alpha_{\mathrm{c}(i)}^2+\sigma_n^2}{M\alpha_{\mathrm{cut}(i)}^2+\sigma_n^2} \\
\mathrm{tr}(\mathrm{R}_{\mathrm{CUT}}^{-1}\mathrm{R}_{\mathrm{c}}) &= \sum_{i=1}^{M}\frac{M\alpha_{\mathrm{c}(i)}^2+\sigma_n^2}{M\alpha_{\mathrm{cut}(i)}^2+\sigma_n^2}
\end{aligned} \tag{10}
$$

and similarily we have equation (11), in which the t^{th} reflection coefficients $\alpha_{\mathrm{cut}(t)}$ and $\alpha_{\mathrm{c}(t)}$ correspond to the t^{th} steering vector which is same as the target's steering vector $\boldsymbol{s}_{\mathrm{t}}$.

Taking (9) and (10) into (6), we have

$$
\begin{aligned}
l=&\mathcal{D}_{\mathrm{KL}}(\mathrm{R}_{\mathrm{CUT}},\hat{\mathrm{R}})-\mathcal{D}_{\mathrm{KL}}(\mathrm{R}_{\mathrm{CUT}},\hat{\mathrm{R}}+\mathrm{R}_{\mathrm{t}}) \\
=&\mathrm{tr}(\mathrm{R}_{\mathrm{CUT}}^{-1}\mathrm{R}_{\mathrm{c}})-\mathrm{tr}(\mathrm{R}_{\mathrm{CUT}}^{-1}(\mathrm{R}_{\mathrm{c}}+\mathrm{R}_{\mathrm{t}})) \\
&+\log(|\mathrm{R}_{\mathrm{CUT}}^{-1}(\mathrm{R}_{\mathrm{c}}+\mathrm{R}_{\mathrm{t}})|)-\log(|\mathrm{R}_{\mathrm{CUT}}^{-1}\mathrm{R}_{\mathrm{c}}|) \\
=&\frac{-M\alpha_{\mathrm{t}}^2}{M\alpha_{\mathrm{cut}(t)}^2+\sigma_n^2}+\log(\frac{M(\alpha_{\mathrm{t}}^2+\alpha_{\mathrm{c}(t)}^2)+\sigma_n^2}{M\alpha_{\mathrm{c}(t)}^2+\sigma_n^2}) \\
=&-\frac{M\alpha_{\mathrm{t}}^2}{M\alpha_{\mathrm{cut}(t)}^2+\sigma_n^2}+\log(1+\frac{M\alpha_{\mathrm{t}}^2}{M\alpha_{\mathrm{c}(t)}^2+\sigma_n^2})
\end{aligned} \tag{12}
$$

During the deduction of (12), we have $\mathrm{tr}(\mathrm{R}_{\mathrm{CUT}}^{-1}\mathrm{R}_{\mathrm{c}}) - \mathrm{tr}(\mathrm{R}_{\mathrm{CUT}}^{-1}(\mathrm{R}_{\mathrm{c}}+\mathrm{R}_{\mathrm{t}})) = -\frac{M\alpha_{\mathrm{t}}^2}{M\alpha_{\mathrm{cut}(t)}^2+\sigma_n^2}$, therefore,

$$
\begin{aligned}
-\frac{M\alpha_{\mathrm{t}}^2}{M\alpha_{\mathrm{cut}(t)}^2+\sigma_n^2} &= \mathrm{tr}(\mathrm{R}_{\mathrm{CUT}}^{-1}\mathrm{R}_{\mathrm{c}})-\mathrm{tr}(\mathrm{R}_{\mathrm{CUT}}^{-1}(\mathrm{R}_{\mathrm{c}}+\mathrm{R}_{\mathrm{t}})) \\
&= -\mathrm{tr}(\mathrm{R}_{\mathrm{CUT}}^{-1}\mathrm{R}_{\mathrm{t}}) \\
&= -\mathrm{tr}(\mathrm{R}_{\mathrm{CUT}}^{-1}\alpha_{\mathrm{t}}^2\boldsymbol{s}_{\mathrm{t}}\boldsymbol{s}_{\mathrm{t}}^{\mathrm{H}}) \\
&= -\alpha_{\mathrm{t}}^2 s_{\mathrm{t}}^{\mathrm{H}}\mathrm{R}_{\mathrm{CUT}}^{-1}s_{\mathrm{t}}
\end{aligned} \tag{13}
$$

and similarly

$$
\frac{M\alpha_{\mathrm{t}}^2}{M\alpha_{\mathrm{c}}^2+\sigma_n^2} = \alpha_{\mathrm{t}}^2 s_{\mathrm{t}}^{\mathrm{H}}\mathrm{R}_{\mathrm{c}}^{-1}s_{\mathrm{t}} \tag{14}
$$

Let (13) and (14) replace the items in (12), the detection formula of the proposed space-time adaptive detector is derived as below.

$$
\Lambda_{\mathrm{PM}} = -\alpha_{\mathrm{t}}^2 s_{\mathrm{t}}^{\mathrm{H}}\mathrm{R}_{\mathrm{CUT}}^{-1}s_{\mathrm{t}} + \log(1+\alpha_{\mathrm{t}}^2 s_{\mathrm{t}}^{\mathrm{H}}\mathrm{R}_{\mathrm{c}}^{-1}s_{\mathrm{t}}) \underset{\mathcal{H}_0}{\overset{\mathcal{H}_1}{\gtrless}} \eta_{\mathrm{PM}} \tag{15}
$$

where Λ_{PM} and η_{PM} are the detection result and threshold of the proposed method (PM). Herein, the estimation result of parameter α_{t} is given by

$$
\alpha_{\mathrm{t}} = \frac{\boldsymbol{s}_{\mathrm{t}}^{\mathrm{H}}\mathbf{R}_{\mathrm{c}}^{-1}\boldsymbol{x}_{\mathrm{CUT}}}{\boldsymbol{s}_{\mathrm{t}}^{\mathrm{H}}\mathbf{R}_{\mathrm{c}}^{-1}\boldsymbol{s}_{\mathrm{t}}} \tag{16}
$$

B. The Application of Proposed Detector in DP-TBD

In this section, we discuss the application of the proposed detector in DP algorithm to implement multi-frame TBD. Assuming there are N_F frames data to detect the target, the objective is to select the target trajectory which is most likely the target track, and output the detection result of N_F frames.

$$
\arg\max_{(T_1,\cdots,T_i,\cdots,T_{N_F})\in\mathcal{S}}\sum_{i=1}^{N_F}\Lambda_i \tag{17}
$$

where T_i, $i = 1\cdots N_F$ is the observed result of the target in i^{th} frame. $\mathcal{S}$ is the ensemble of all physically feasible trajectories. Λ_i, $i = 1\cdots N_F$ is the output of the output of the detector. Herein, it should be pointed out that the unknown target motion state would cause difficulty and calculation burden for the multi-frame processing. To solve this problem, the kinematics boundary constraint (KBC) is utilized to restrict the velocity maximum of the target between different frames [26], namely

$$
r_{m-1} - v_{\max}t \leqslant r_m \leqslant r_{m-1} + v_{\max}t \tag{18}
$$

where r_i, $i = 1, \cdots, N_F$ is the range of target in each frame. $v_{\max}$ is the maximum tracking speed of the target, t is the time interval between frames.

Formula (18) restricts the target state transition from frame to frame, thus reducing the complexity of implementing DP-TBD. However, as observed in (15), the target speed information can be obtained while detecting the target. Although the speed of the target given by the normalized Doppler in $\boldsymbol{s}_{\mathrm{t}}$ is not accurate enough, the associated region can be effectively reduced, and the boundary constraint of the proposed method between frames is

$$
r_{m-1} + vt - \Delta \leqslant r_m \leqslant r_{m-1} + vt + \Delta \tag{19}
$$

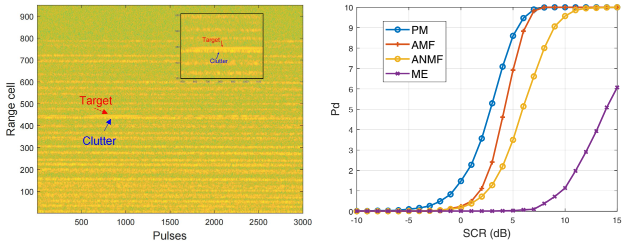

(a) Raw data (b) Pd curves

Fig. 1. The raw data and Pd curves under different SCRs.

where v is the speed of the target estimated by Doppler information and Δ is the fault tolerance value. Different from (18), the proposed formula (19) obeys the Doppler boundary constraint (DBC).

Detailedly, the processing procedures of the proposed 2S-IG detector are outlined in Algorithm 1.

Algorithm 1 The processing procedures of the proposed 2S-IG detector

Input:

The received radar pulse data of N_F successive frames.

Output:

The detection result and estimated target trajectory.

1: for k=1:N_F do
2: Compute the test statistic in (15).
3: Solve the optimization problem (17), in which $\mathcal{S}$ is determined by formula (19).
4: end for
5: Compare the maximum of the merit function $\sum_{i=1}^{N_F} \Lambda_i$ with a given threshold of multi-frame detection.
6: Return the prospective trajectory of N_F frames recursively.

IV. Experimental Results and Analysis

This section carries out the experiments of performance evaluation by using real radar data. The experiments is based on the sea-detecting data-sharing program (SDDSP) data measured by the Naval Aeronautical University and includes two parts. First, a simulated target is added to the measured clutter data to verify the advantageous performance of the proposed detector (PM). Then, in the second part, the weak moving cooperative target in the dataset is considered, and the performance of various DP-TBD algorithms are analyzed.

The datafile used in this section is $27520221112175025\_stare\_VV.mat$. The data was collected by the X-band TianAo SPPR50P-VV radar which works in 9.3–9.5 GHz. As shown in Fig 1a, the sea clutter is greatly heterogeneous and there are many waves that can easily cause false alarms and false tracks.

In this paper, the competitive AMF, ANMF, MIG detector and maximum eigenvalue (ME) detector are employed as comparison methods. First, the data from range cell 500 to 900 are selected to compare the performance of various detectors.

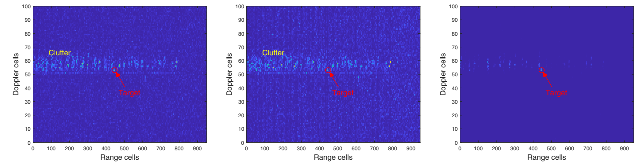

(a) AMF (b) ANMF (c) PM

Fig. 2. The detection result of real target.

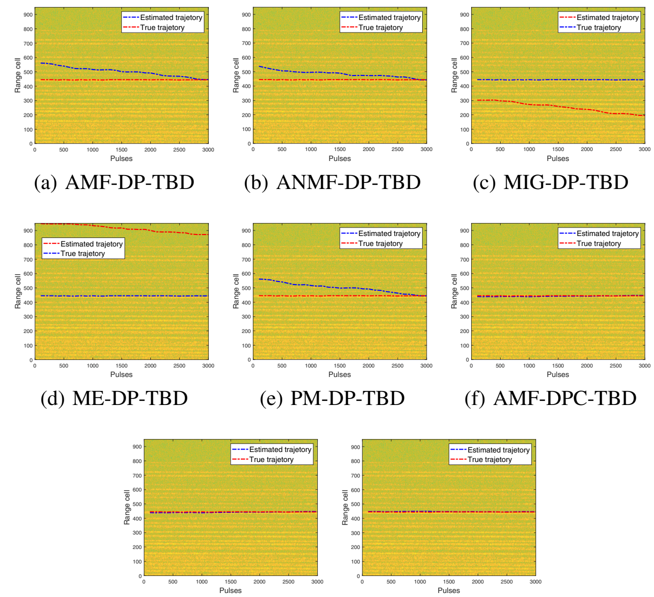

(a) AMF-DP-TBD (b) ANMF-DP-TBD (c) MIG-DP-TBD

(d) ME-DP-TBD (e) PM-DP-TBD (f) AMF-DPC-TBD

(g) ANMF-DPC-TBD (h) PM-DPC-TBD

Fig. 3. The multi-frame detection results of real target.

A echo response $\boldsymbol{s} = \alpha \boldsymbol{p}$ is added, where $\boldsymbol{p}$ is the steering vector of the simulated target and α is the signal amplitude control factor determined by SCR. The normalized Doppler of simulated target is set to 0.25. Fig 1b shows the probability of detection (Pd) curves of different detectors and we can see that the proposed method has the best detection performance, especially when low SCR target appears. Herein, the detection threshold is calculated by 10^5 Monte Carlo experiments and the false alarm rate is 10^{-4}. The number of reference cells is 64 and $M = 10$.

Then, various DP-TBD algorithms are performed to discuss the detection performance of the measured slowly-moving target. The target is a sea buoy moving with the waves and located at the range cell from 441 to 453. It's worth indicating that the target is adjacent to the clutter, making a great challenge to detectors. Fig 2 presents the range-Doppler maps of different detections, the proposed method succeeds in detecting the target and suppresses the heterogeneous strong clutter better.

Furthermore, we discuss the multi-frame detection results of the real target. In this experiment, the first 3s (30 frames and 100 pulses per frame) of the data are utilized for the validation. Based on the conventional KBC DP-TBD method,

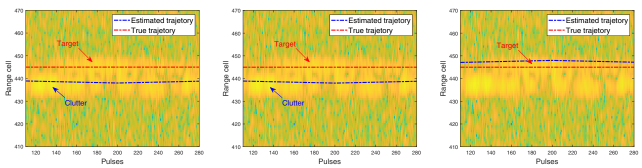

(a) AMF-DP-TBD (b) ANMF-DP-TBD (c) MIG-DP-TBD

Fig. 4. Local map of the multi-frame detection trajectory.

the multi-frame detection result of the proposed method and comparison algorithms are presented from Fig 3a to Fig 3e. We can see that all these algorithms fail to detect the target in strong clutter background, but the proposed method, AMF and ANMF detector have the minimum trajectory deviation. Then we consider the proposed DBC multi-frame detection algorithm introduced in section III-B. As shown from Fig 3f to Fig 3h, the proposed DBC method effectively improves the detection performance. The mean absolute error (MAE) of DBC detection are listed in Table I, indicating that the proposed PM-DPC-TBD method has the best performance. Herein, it should be emphasized that although the tracks output by the AMF and ANMF detectors are close to the truth, they are still false tracks, as illustrated in Fig 4. Actually, part of the trajectory output by the AMF and ANMF detectors belongs to the sea clutter adjacent to the target, thus the target is not completely detected. Whereas, the proposed method does not suffer such a problem, as shown in Fig 4c.

TABLE I
OUTPUT MAE OF DIFFERENT DBC-TBD ALGORITHMS

Method	PM-DBC-TBD	AMF-DBC-TBD	ANMF-DBC-TBD
MAE	2.16	3.56	3.4

V. CONCLUSION

In this paper, we proposed a DP-TBD method for airborne multi-channel radar to treat the problem of weak moving target detection. Firstly, a novel information geometry-based space-time adaptive detector is proposed. Then, based on the DP-TBD algorithm, we discuss the application of the proposed detector in multi-frame detection. The proposed DBC-DP-TBD method utilizes the Doppler information rather than the KBC to output the trajectory, thus it achieves advantageous performance in multi-frame detection. The experiment results illustrate the outstanding performance of the proposed detector.

REFERENCES

[1] Guerci, J.R. Space-time Adaptive Processing for Radar, 2nd ed.; Artech House: Fitchburg, MA, USA, 2015; pp. 1–9.

[2] J. Ward. “Space-Time Adaptive Processing for Airborne Radar,” *Technical Report TR-1015*, MIT Lincoln Laboratory: Lexington, MA, USA, 1994

[3] I.S. Reed, J.D. Mallett, L.E. Brennan.“Rapid Convergence Rate in Adaptive Arrays,” *IEEE Trans. Aerosp. Electron. Syst.*, vol. 10, pp. 853-863, Nov. 1974.

[4] X. Chen, Y. Cheng, H. Wu and H. Wang. “Heterogeneous Clutter Suppression for Airborne Radar STAP Based on Matrix Manifolds,” *Remote Sensing*, vol. 13, no. 16, pp. 3195, Aug. 2021.

[5] Z. Yang, Y. Cheng, H. Wu, et al. ”Maximum-Eigenvalue-Based Multi-frame Track-Before-Detect Method for Weak Moving Target Detection,” *IEEE Trans. Aerosp. Electron. Syst.*, vol. 61, pp. 8081-8090, Jun. 2025.

[6] W. Liu, J. Liu, Y. Gao, et al. “Multichannel signal detection in interference and noise when signal mismatch happens,” *Signal Processing*, vol. 166, pp. 107268, Jan. 2020.

[7] Kelly E J. “An Adaptive Detection Algorithm,” *IEEE Trans. Aerosp. Electron. Syst.*, vol. 22, pp. 115–127, 1986.

[8] W. Chen, I.S. Reed. “A New CFAR Detection Test for Radar,” *Digital Signal Processing*, vol. 1, pp. 198-214, 1991.

[9] Conte E., Lops M., Ricci G., et al. “Adaptive Detection Schemes in compound-Gaussian Clutter,” *IEEE Trans. Aerosp. Electron. Syst.*, vol. 34, no. 4, pp. 1058-1069, 1998.

[10] W. Liu, W. Xie, J. Liu, et al. “Adaptive double subspace signal detection in Gaussian background—part. I: Homogeneous environments,” *IEEE Trans. Sign. Process.,* vol. 62, no. 9, pp. 2345-2357, 2014.

[11] W. Li, Q. Miao, Y. Yuan, et al. ”Automotive Radar Multi-Frame Track-Before-Detect Algorithm Considering Self-Positioning Errors,” *IEEE Trans Intell. Transp. Syst.*, early access, DOI: 10.1109/TITS.2025.3565733.

[12] D. Orlando, L. Venturino, M. Lops and G. Ricci, ”Track-Before-Detect Strategies for STAP Radars,” *IEEE Trans. Sign. Process.*, vol. 58, no. 2, pp. 933-938, Feb. 2010.

[13] D. Orlando, G. Ricci and Y. Bar-Shalom, ”Track-Before-Detect Algorithms for Targets with Kinematic Constraints,” *IEEE Trans. Aerosp. Electron. Syst.*, vol. 47, no. 3, pp. 1837-1849.

[14] W. Li, Y. Wei, K.C. Teh, and L. Kong, ”Radar Multiframe Detection in a Complicated Multitarget Environment,” *IEEE Trans. Geosci. Remote Sens.*, vol. 61, pp. 1-16, 2023.

[15] W. Li, Y. Wei, L. Kong and K.C. Teh,, ”An Efficient Track-Before-Detect for Multi-PRF Radars with Range and Doppler Ambiguities,” *IEEE Trans. Aerosp. Electron. Syst.*, vol. 58, pp. 4083-4100, Mar. 2022.

[16] W. Li, Y. Wei, K.C. Teh, and L. Kong, ”Adaptive Multiframe Detection Algorithm With Range-Doppler-Azimuth Measurements,” *IEEE Trans. Geosci. Remote Sens.*, vol. 60, pp. 1-16, 2022.

[17] M. S. Arulampalam, S. Maskell, N. Gordon, and T. Clapp. ”A tutorial on particle filters for online nonlinear/non-gaussian bayesian tracking,” *IEEE Trans. Sign. Process.*, vol. 50, no. 2, pp. 174–188, 2002.

[18] L. R. Moyer, J. Spak, and P. Lamanna. ”A multi-dimensional hough transform-based track-before-detect technique for detecting weak targets in strong clutter backgrounds,” *IEEE Trans. Aerosp. Electron. Syst.*, vol. 47, no. 4, pp. 3062–3068, 2011.

[19] W. Yi, L. Kong, J. Yang, et al. ”A tracking approach based on dynamic programming track-before detect,” In 2009 IEEE Radar Conference. IEEE, 2009, pp. 1–4.

[20] H. Wu, Y. Cheng, X. Chen, et al. “Information Geometry-Based Track-Before-Detect Algorithm for Slow-Moving Fluctuating Target Detection,” *IEEE Trans. Sign. Process.*, vol. 71, pp. 1-16, 2023.

[21] R. Zou, Y. Cheng, H. Wu, et al. “A Two-Step Space-Time Adaptive Matrix Information Geometry Detector for Multi-Channel Radar,” *IEEE Trans. Aerosp. Electron. Syst.*, early access, DOI: 10.1109/TAES.2025.3566056.

[22] H. Wu, Y. Cheng, X. Chen, et al. ”Power Spectrum Information Geometry-Based Radar Target Detection in Heterogeneous Clutter,” *IEEE Trans. Geosci. Remote Sens.*, vol. 62, pp. 1-16, Jan. 2024.

[23] R. Zou, Y. Cheng, H. Wu, et al. “Radar Target Detection in Heterogeneous Environment Based on HPD Manifold Clustering,” *IEEE Geosci. Remote Sens. Lett.*, vol. 21, pp. 1-5, 2024.

[24] R. Zou, Y. Cheng, H. Wu, et al. “A Steering-vector-based Matrix Information Geometry Method for Space-time Adaptive Detection in Heterogeneous Environment”, *Remote Sensing*, vol. 16, no. 12, pp. 2208, 2024.

[25] Z. Wang, Y. Wang, K. Duan, et al. “Subspace-Augmented Clutter Suppression Technique for STAP Radar,” *IEEE Geosci. Remote Sens. Lett.*, vol. 13, pp. 1-5, 2016.

[26] D. Orlando, G. Ricci and Y. Bar-Shalom, ”Track-Before-Detect Algorithms for Targets with Kinematic Constraints,” *IEEE Trans. Aerosp. Electron. Syst.*, vol. 47, no. 3, pp. 1837-1849.